Biointerphases (2012) 7:56
DOI 10.1007/s13758-012-0056-4

ARTICLE

Development of a Tuned Interfacial Force Field Parameter Set for the Simulation of Protein Adsorption to Silica Glass

James A. Snyder · Tigran Abramyan · Jeremy A. Yancey · Aby A. Thyparambil · Yang Wei · Steven J. Stuart · Robert A. Latour

Received: 20 July 2012 / Accepted: 13 August 2012 / Published online: 1 September 2012

Abstract Adsorption free energies for eight host–guest peptides (TGTG-X-GTGT, with X = N, D, G, K, F, T, W, and V) on two different silica surfaces [quartz (100) and silica glass] were calculated using umbrella sampling and replica exchange molecular dynamics and compared with experimental values determined by atomic force microscopy. Using the CHARMM force field, adsorption free energies were found to be overestimated (i.e., too strongly adsorbing) by about 5–9 kcal/mol compared to the experimental data for both types of silica surfaces. Peptide adsorption behavior for the silica glass surface was then adjusted using a modified version of the CHARMM program, which we call *dual force-field* CHARMM, which allows separate sets of nonbonded parameters (i.e., partial charge and Lennard-Jones parameters) to be used to represent intra-phase and inter-phase interactions within a given molecular system. Using this program, interfacial force field (IFF) parameters for the peptide-silica glass systems were corrected to obtain adsorption free energies within about 0.5 kcal/mol of their respective experimental values, while IFF tuning for the quartz (100) surface remains for future work. The tuned IFF parameter set for silica glass will subsequently be used for simulations of protein adsorption behavior on silica glass with greater confidence in the balance between relative adsorption affinities of amino acid residues and the aqueous solution for the silica glass surface.

J. A. Snyder · T. Abramyan · J. A. Yancey · A. A. Thyparambil · Y. Wei · R. A. Latour (✉)
Department of Bioengineering, 501 Rhodes Engineering Research Center, Clemson University, Clemson, SC 29634, USA
e-mail: LatourR@clemson.edu

S. J. Stuart
Department of Chemistry, 369 Hunter Laboratories, Clemson University, Clemson, SC 29634, USA

1 Introduction

The adsorption behavior of proteins on material surfaces serves an important role for numerous applications in the fields of biomaterials and biotechnology, including the design of implants for improved biocompatibility [1–4], drug delivery systems [5, 6], biosensors [7, 8], and surfaces used for bioseparations [9]. There is also considerable interest in the interactions of proteins with material surfaces for applications related to biodefense [10–12]. For example, in the event of a bioweapons attack involving the release of a protein toxin, such as ricin, protein-surface interactions will mediate the adhesion of the toxin to exposed environmental surfaces, with an understanding of protein–surface interactions then being important for the design of safe and effective wash agents for surface decontamination and agent deactivation. Furthermore, because proteins mediate the adhesion of other biological entities to surfaces [12], including bacteria, viruses, and fungi, a molecular-level understanding of protein-surface interactions is important for the design of decontamination strategies for these types of biological agents as well.

The bioactive state of an adsorbed protein is largely determined by the orientation and conformation of the protein on the surface, and thus methods are needed to understand and predict these types of interactions. Over the past three decades, molecular dynamics (MD) simulations using empirical force field-based methods have been developed as a valuable tool for the prediction of the conformational behavior of proteins in aqueous solution. These methods have similar potential for use in predicting the orientation, conformation, and bioactivity of proteins when adsorbed on material surfaces. However, before this potential can be realized, it is essential that these computational methods be first developed, evaluated, and

validated against experimental data in order to confirm that they are able to realistically represent protein–surface interactions.

While numerous experimental [13–16] and computational studies [17–19] on interfacial interactions with quartz and silica glass have previously been published, there is a lack of experimental data sets providing quantitative values that can be used to design empirical force field parameters for the simulation of peptide and protein adsorption behavior to silica surfaces [20]. While detailed studies have been conducted to establish force field parameters for the interactions of water molecules with both quartz and silica glass surfaces [21–23], these same parameter sets cannot necessarily be trusted to accurately represent the competitive adsorption behavior between amino acid residues of peptides and proteins and water for these same surfaces because protein force fields themselves have not been parameterized for amino acid adsorption behavior, and may not be accurate [24]. Ab initio methods have been used to develop parameters to address protein adsorption behavior based on individual amino acids or small chemical analogs [25–27], but the current limitations of these methods for adequately representing adsorption behavior in aqueous solution raises concerns about the accuracy of parameters obtained in this manner. At this time, therefore, the most reliable way to confidently develop force field parameters to accurately represent peptide and protein adsorption behavior is to have carefully chosen experimental data to which force field-based simulation results can be directly matched and quantitatively compared. Only then can the force field parameterization be directly and confidently assessed and tuned in order to capture the correct balance between the relative interactions of amino acid residues and solvent molecules (i.e., water and soluble ions) with the surface, achieving the ultimate goal of being able to accurately predict peptide and protein adsorption behavior through empirical force field-based molecular simulations.

As a first step towards accurate simulation of protein adsorption behavior, the interactions between the individual amino acids that make up a protein and the functional groups presented by a surface must be accurately represented within an aqueous environment. One property that can provide a quantitative measure of amino acid-surface interactions, which is directly accessible both experimentally and from MD simulations, is adsorption free energy. In previous work, we have developed experimental methods using a combination of surface plasmon resonance spectroscopy (SPR) [28, 29] and atomic force microscopy (AFM) [30, 31] to characterize the standard-state Gibbs adsorption free energy (ΔG°_{ads}) using host–guest peptides. We also then developed MD simulation methods using biased-energy replica exchange molecular dynamics (biased-REMD) for the calculation of standard state Helmholtz adsorption free energy (ΔA°_{ads}) for comparison with our experimental results [32, 33]. (Under aqueous solution conditions, the difference between Gibbs and Helmholtz free energies is negligible, due to the near incompressibility of liquid water.)

In recent studies, we conducted experimental SPR [28, 29] and biased-REMD simulations [24] to measure and calculate adsorption free energy, respectively, for small host–guest peptides with a sequence of TGTG-X-GTGT (X = V, T, D, F, and K amino acids using the standard one-letter amino acid code) over nine different functionalized alkanethiol self-assembled monolayer (SAM) surfaces in aqueous solution. The ΔA°_{ads} values calculated from the biased-REMD simulations, which were performed using the CHARMM22/CMAP protein force field [34, 35], were then compared with the experimental values to assess the level of agreement. The results of these comparisons showed that the adsorption free energy values for several of the peptide-SAM systems obtained using the CHARMM force field deviated from the experimental values by more than 1.0 kcal/mol, which we take as a general criterion for acceptable accuracy based on the degree of certainty of the experimental methods. These results thus indicated the need to adjust the CHARMM force field parameters to more adequately represent amino acid-surface interactions before these methods could be further extended in an attempt to accurately simulate protein adsorption behavior. In order to address this need, we subsequently modified the CHARMM molecular simulation program to enable nonbonded force field parameters controlling amino acid–SAM surface interactions (i.e., the van der Waals (vdW) and electrostatic interactions) to be independently modified while still enabling the standard CHARMM22/CMAP force field to be used to represent the conformational behavior of a peptide in solution, for which purpose it was primarily developed. We call this modified CHARMM program *dual force field* (Dual-FF) CHARMM [36]. Using the Dual-FF CHARMM program, we demonstrated that the nonbonded force field parameters controlling solution–surface interactions can be modified independently of the solution–solution parameters, resulting in an interfacial force field (IFF) with adsorption free energies that closely match experimental values, while leaving the peptide's conformational behavior in solution unperturbed.

In the current study, we have performed a similar set of simulations and peptide adsorption free energy calculations for TGTG-X-GTGT host–guest peptides over two types of silica surfaces (quartz (100) and silica glass) in order to extend our capabilities beyond the use of relatively simple model SAM surfaces. The ΔA°_{ads} values obtained for

peptide adsorption to this type of surface using published CHARMM parameters for silica surfaces are greatly overestimated (i.e., peptides adsorb much too strongly) relative to experimental values for each of the eight different host–guest peptides. Nonbonded parameters were then modified using our Dual-FF CHARMM program to bring the calculated ΔA°_{ads} values for each peptide to within about 0.5 kcal/mol agreement of the experiment data on silica glass. The quartz (100) system remains for future work.

2 Methods

2.1 Experimental Determination of Peptide Adsorption Free Energy on Silica Surfaces

In previous studies we have shown that desorption forces measured by AFM for TGTG-X-GTCT peptides (linked to the AFM tip using polyethylene–glycol (PEG) tethers by the cysteine (C) amino acid residue) are well correlated with adsorption free energies for TGTG-X-GTGT peptides as determined using SPR [30, 31]. This AFM technique was developed to provide a means to determine effective adsorption free energies of peptides on material surfaces that are not conducive to SPR. In this present study, we implemented our standardized AFM method to determine the effective adsorption free energy of TGTG-X-GTGT peptides on both quartz (100) and silica glass surfaces. Specific details of this method have been previously published [30, 31] and they are briefly described below for the present set of studies.

2.1.1 Materials: Peptides, Silica Surfaces, and Solution Conditions

These studies were carried out for a set of eight guest amino acid residues with X = V, F, T, W, G, N, D, and K (synthesized by Biomatik, Wilmington, DE; characterized by analytical HPLC and mass spectral analysis to have at least 98 % purity). These guest residues were selected to include representatives from each characteristic class of amino acid: nonpolar aliphatic, aromatic, polar, negatively charged, and positively charged. The adsorbent surfaces used for these AFM studies were quartz plates with a (100) surface plane (MTI Corporation, Richmond, CA) and fused silica glass plates (Chemglass Life Sciences, Vineland, NJ). For our standard cleaning procedures, the adsorbent surfaces were cleaned by sonicating (Branson Ultrasonic Corporation, Danbury, CT) in (a) "piranha" [7:3 (v/v) H_2SO_4 (Fisher Scientific, Fair Lawn, NJ)/H_2O_2 (Fisher Scientific, Fair Lawn, NJ, USA)], and (b) basic solution [1:1:3 (v/v/v) NH_4OH (Fisher Scientific, Fair Lawn, NJ, USA)/H_2O_2/H_2O] at 50 °C for 1 min. After each stage of the washing process, the substrates were rinsed in absolute ethanol and nanopure water and dried under a steady stream of nitrogen gas (National Welders Supply Co., Charlotte, NC, USA). Prior to use, surfaces were cleaned by sonication (Branson Ultrasonic Corp., Danbury, CT) at room temperature for 30 min in 0.3 vol.% Triton X-100 (Sigma Chemical Co., St. Louis, MO), rinsed with absolute ethanol and nanopure water, and characterized by static water contact angle (CAM 200, KSV Instruments, Monroe, CT) and X-ray photoelectron spectroscopy (XPS), with values all falling within the expected ranges for clean surfaces with the appropriate chemical composition (see Table 1) [30, 37–42]. Peptide desorption forces from the silica surfaces were measured at room temperature in 10 mM potassium phosphate buffered water (PPB; 2 mM KH_2PO_4, 8 mM K_2HPO_4 in nanopure water; pH 7.4; Fisher Scientific, Fair Lawn, NJ).

2.1.2 Desorption Force Measurement and Correlation to Adsorption Free Energy

Per our standardized protocol [35, 36], AFM studies were conducted using an MFP-3D instrument (Asylum Research, Santa Barbara, CA) with DNP-10 silicon nitride cantilevers

Table 1 Surface characterization: atomic composition and static contact angle analyses for each surface used in this study

Surface moiety	C (%)	S (%)	N (%)	O (%)	Si (%)	Contact angle (°)
Fused glass**	25.0 (2.0)	*	<1.0	49.0 (2.0)	22.0 (1.0)	23 (4)
Quartz (100)	15.0 (2.0)	<1.0	<2.0	53 (1.0)	30.0 (3.0)	13 (3)

An asterisk (*) indicates negligible value for atomic composition data. (Mean ± 95 % confidence interval, N = 3.)

The presence of extra carbon composition is believed to be originating from surface contamination due to the exposure of samples to air after cleaning. These are the typical adventitious and unavoidable hydrocarbon impurities that adsorb spontaneously from ambient air onto the glass and quartz surface. However, since the surface carbon content also correlates strongly with the static water contact angle [38], our static water contact angle measurements show 23° for fused glass and 13° for quartz, which is quite comparable with expected values for clean silica substrates reported by many other groups [39–42], thus providing a good indicator that our standard cleaning protocol was effective

** Fused glass slide also contains Zn (<1 %) and Al (<1 %)

(Veeco Nanofabrication Center, Camarillo, CA). The tips were amino-functionalized by incubating them overnight in a 55 % (wt/vol) solution of ethanolamine chloride (Sigma Chemical Co., St. Louis, MO) in dimethyl sulfoxide (DMSO) at room temperature in the presence of 0.3 nm molecular sieve beads and subsequently washed in DMSO and ethanol, and dried under nitrogen gas. The host–guest peptides were then tethered to the AFM tips by a heterobifunctional polyethylene glycol tethering agent with amine functionality at one end for linking to the AFM tips and a thiol group at the other for linking to the cysteine residues of the peptides (3.4-kDa (ortho-pyridyl)disulfide-poly(ethylene-glycol)-succinimidyl ester (OPSS-PEG-NHS), Creative PEGWorks, Winston Salem, NC). Tips functionalized with hydroxyl-terminated PEG chains (PEG–OH; i.e., without peptide) were used as controls (i.e., non-adsorbing system).

Peptide desorption force (F_{des}) was measured by bringing the functionalized AFM tip with the tethered peptide (or PEG-OH controls) in contact with the silica surfaces for one second of surface delay and then retracting the tip at a constant vertical scanning speed of 0.1 μm/s. The interaction force trace was recorded versus as a function of the tip–sample surface separation distance, from which F_{des} values were measured. For each of the peptide–surface systems, two different substrate samples from the same material were used, and force measurements were performed at three or more distinct sites on each substrate. A minimum of ten force–separation curves was recorded at each site. In total, more than 60 force–separation curves were used to generate a histogram from which the mean value of F_{des} was determined. Effective values of the standard-state adsorption free energy (ΔG°_{ads}) were then estimated from our previously validated F_{des} versus ΔG°_{ads} correlation plot [30] for each peptide–surface system for direct comparison with adsorption free energy values calculated from molecular simulation.

2.2 Molecular Simulation Studies

2.2.1 *Model Construction and Equilibration*

All MD simulations were performed using the CHARMM molecular simulation software [34, 35, 43]. In accordance with the experimental studies, simulations were performed to calculate adsorption free energies for TGTG-X-GTGT host–guest peptides with X = V, F, T, W, G, N, D, and K on quartz (100) and silica glass surfaces. The host–guest peptides were modeled using the CHARMM22 protein force field [34] with CMAP correction [35]. Two different types of silica surface were modeled in this study: a crystalline quartz surface and an amorphous silica (i.e., silica glass) surface. The molecular model of the quartz was developed using the coordinates of the unit cell for a (100) surface plane [21] from which a square-shaped quartz unit cell was generated that was approximately 50 Å on each side and 15 Å thick. The initial molecular model for the silica glass surface was generously prepared for us by Dr. Chris Lorenz of King's College, University of London, using the Large-scale Atomic/Molecular Massively Parallel Simulator (LAMMPS) software package [44, 45]. The initial silica surface models were each then further modified for use with the CHARMM molecular simulation program using CHARMM PATCH commands for creating bonds, bond angles, and dihedral angles for atoms crossing the primitive and adjacent image cells, to represent an infinite surface plane. The quartz surface was terminated by geminal silanol groups [$>Si(OH)_2$] on the top (hydrophilic) and by $Si-H_2$ on the bottom (hydrophobic). The top and bottom surfaces of the silica glass were terminated by silanol groups (Si–OH) as necessary to provide four bonds per Si atom. Published sets of CHARMM force field parameters, which were specifically designed for silica interactions with TIP3P water, were initially used for both the quartz [21] and silica glass [23] surfaces. The remainder of each system was simulated using standard CHARMM22/CMAP protein force field parameters.

A water layer (~35 Å thick) constructed using CHARMM's TIP3P water was initially placed on the top of the silica surfaces and an additional 15 Å water layer with waters kept fixed was placed between the bottom surface and the adjacent top water layer to prevent interaction of the peptide with the image of the bottom of the silica surface layer when periodic boundary conditions were applied. The two water layers were first separately equilibrated in the isothermal-isobaric (*NPT*) ensemble at 298 K and 1 atm for 500 ps using the Leapfrog integrator. The 15 Å layer was then allowed to equilibrate with the bottom surface for 1.0 ns, after which the coordinates of these waters were kept fixed during all subsequent simulations. The host–guest peptide TGTG-X-GTGT was then introduced into the top water layer and overlapping waters were deleted. Only the surface hydroxyl O and H atoms on the top surface were allowed to move freely during dynamics. All other atoms of the silica surfaces were kept fixed for computational efficiency. One Na^+ or Cl^- counter-ion was added to systems with X = K, or D to maintain overall charge neutrality. Representative illustrations of model systems for the TGTG-X-GTGT peptide over the quartz (100) and silica glass surfaces are provided in Fig. 1.

After initial model construction, the length of the simulation cell along the *z*-axis direction (normal to the surface plane) was adjusted so as to establish 1 atm pressure conditions for the aqueous solution above the surface. This was accomplished using a technique previously developed by our group that is based on the calculation of an effective

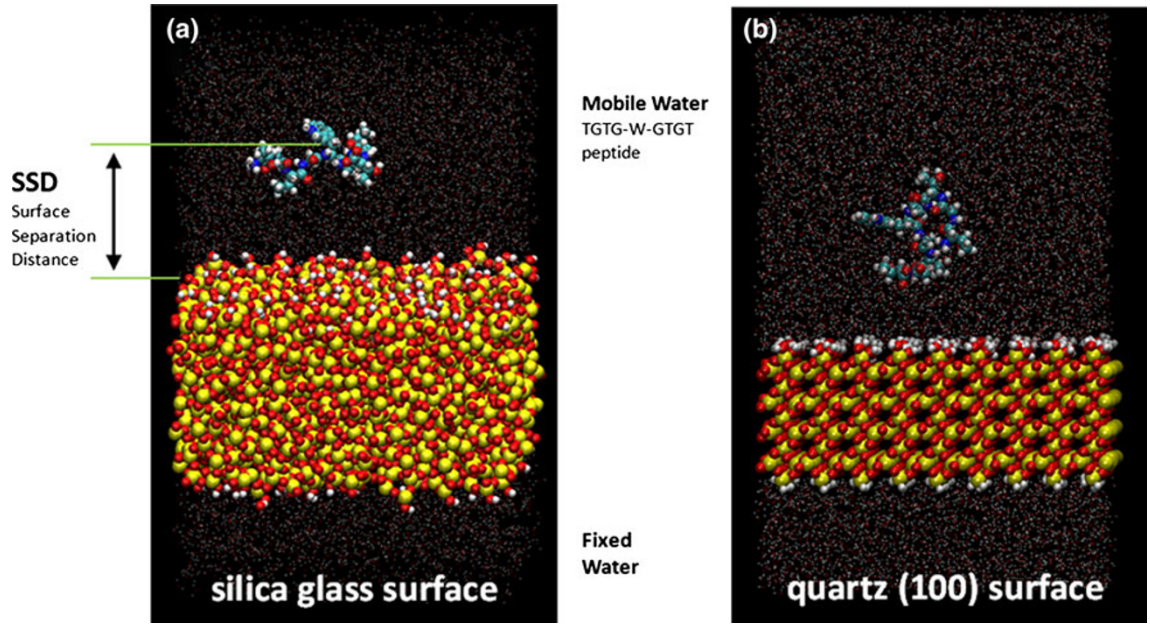

Fig. 1 Model of host-guest peptide TGTG-W-GTGT over (**a**) a silica glass surface and (**b**) a quartz (100) surface. Both mobile and fixed water layers are shown as points for clarity. The specific systems shown consist of 16,485 and 18,576 atoms, respectively

virial per atom value for a defined 'slab' of the bulk-solution phase of the system well above the solid–liquid interface [46]. In previous studies, we determined that this step was necessary because pressure values reported by molecular simulation programs for molecular models with fixed atoms are susceptible to large errors, which can substantially affect the calculated values of adsorption free energy [46]. Accordingly, the height of the water box for our molecular models was adjusted until the effective virial per atom for a slab of bulk solution matched a value corresponding to 1 atm solution conditions.

Following model construction, each solvated host–guest peptide/silica system was subjected to 100 ps of heating from 0 to 298 K, followed by 4 ns of dynamics in the canonical (*NVT*) ensemble with the peptide unrestrained in preparation for conducting the production simulations for the calculation of peptide adsorption free energy. For these and all subsequent MD simulations, we used the modified velocity Verlet integrator (VV2) and a Nosé-Hoover thermostat [47, 48] with the time-step set to 2 fs. The van der Waals interactions were represented using the 12-6 Lennard-Jones potential with a group-based force-switched cutoff that started at 8 Å and ended at 12 Å with a pair-list generation cutoff at 14 Å. Bonds involving hydrogen atoms were constrained using the RATTLE [49] algorithm.

2.2.2 *Calculation of Peptide Adsorption Free Energy*

In order to perform sufficient sampling for the calculation of peptide adsorption free energy to our silica surfaces, we use a combination of umbrella sampling and biased-REMD advanced sampling methods, which our group previously developed for this purpose [24, 32, 33]. The biased-REMD method combines two advanced sampling strategies in a single simulation. A biased-energy function enables the peptide to escape from a strongly adsorbing surface, thus preventing problems that occur when the full range of surface–separation distances (SSD) are not sampled [50]. Simultaneously, the REMD simulation uses multiple replicas at elevated temperatures to enhance conformational sampling of the peptide [51]. While the use of either of these advanced sampling methods alone does not provide adequate sampling for the accurate calculation of adsorption free energy, their combined use enables both sampling problems to be efficiently overcome in a single simulation [24, 32, 33], thus enabling adsorption free energy to be properly determined.

In order to calculate ΔA°_{ads} from our simulations, the biasing function was first derived using windowed umbrella sampling [52–56] along the SSD reaction coordinate. For this method, a series of harmonic restraining potentials was applied to force the peptide to sample the full SSD coordinate space between 3 and 25 Å. These potentials have the form:

$$V_u = 0.5\, k_u(\mathrm{SSD} - \mathrm{SSD}_0) \quad (1)$$

where k_u is the force constant and SSD_0 is the reference point on the SSD coordinate about which the center of mass of peptide was restrained to ensure enhanced sampling within each SSD window. For the umbrella sampling

simulations, a force constant of 2 kcal mol^{-1} $Å^{-2}$ was used for the harmonic restraining potential. An equilibration period of 1–3 ns was performed at 298 K in the canonical (*NVT*) ensemble with the restraining potential applied prior to production runs from which sampling data was collected. The resulting trajectories from the umbrella sampling simulations were then analyzed using the weighted histogram analysis method (WHAM) [57] to calculate a potential of mean force (PMF) as a function of SSD, which also represents the adsorption free energy profile. The resulting PMF profile was then fit to a Derjaguin, Landau, Verwey, and Overbeek (DLVO) potential [58], modified by the addition of optional Gaussian functions where necessary to provide a better fit to the PMF profile. The negative of this fitted analytical function was then added to the force field equation as a biasing potential for subsequent biased-REMD simulations. This procedure enables the peptide to escape from a strongly adsorbing surface during the REMD simulation, in order to adequately sample the position of the peptide over the full SSD coordinate space while also providing full sampling of the peptide's conformational space for the proper calculation of ΔA_{ads}. We note that it is not necessary that the PMF be fully and accurately converged in these umbrella sampling simulations, merely converged well enough to allow the peptide to escape confinement on the surface when used as a biasing potential during the biased REMD simulation. After conducting a biased-REMD simulation, the resulting biased SSD-position probability density profile was corrected using statistical mechanics principles and the probability-ratio method [59] to remove the effects of the applied biasing function to give an unbiased probability distribution using Eq. 2 [24]:

$$\frac{P_i}{P_b} = \frac{\overline{P_i}}{\overline{P_b}} \exp\left[\frac{(V_B)_i}{RT}\right] \qquad \frac{P_i}{P_b} = \frac{\overline{P_i}}{\overline{P_b}} \exp\left[\frac{(V_B)_i}{RT}\right] \tag{2}$$

where P and $\overline{p}$ are the non-biased and biased probability densities, subscripts 'i' and 'b' denote positions within the interfacial and bulk solution regions of the system, $(V_B)_i$ represents the biasing function at SSD position 'i', and R and T represent the ideal gas constant and absolute temperature of the system, respectively.

Using the resulting unbiased probability distribution, a value for the adsorption free energy was calculated using the expression [24]:

$$\Delta A_{ads} = -RT \ln\left[\frac{W}{\delta P_b}\sum_{i=1}^{N} P_i\right] \tag{3}$$

where subscripts 'i' and 'b' denote interfacial and bulk solution regions of the system, P_i and P_b are the probabilities of the peptide being at positions SSD_i, and SSD_b, respectively, with SSD_b defined to be the distance from the surface for which peptide-surface interactions become negligibly small, which for these systems is typically beyond 15 Å from the surface plane. N is the number of bins that partition the SSD coordinate space for which $P_i < P_b$, δ is the theoretical thickness of the adsorbed layer [24, 29], and W is the bin width used to produce the probability distribution. ΔA°_{ads} values for the interaction of each host–guest peptide on the silica surfaces were thus determined from simulations for comparison with the experimental results obtained from the experimental AFM studies for these same systems as a direct means of assessing the accuracy of the force field that was used in the simulations. More detailed explanation of these methods can be found in our previous papers [24, 32, 33].

Biased-REMD simulations were performed using a set of 24 replicas at 24 temperatures exponentially distributed over the range of 298–400 K. A set of 24 initial random configurations was used for the REMD calculations to facilitate conformational sampling. These conformations were obtained from the final configurations of the windowed umbrella sampling simulations that were performed prior to conducting the REMD simulations. MD simulations for each replica were first run for 120 ps with no exchanges permitted to allow each replica to equilibrate to its designated temperature. Biased-energy REMD production simulations were then run for 10 ns, with exchanges attempted every 1.0 ps between adjacent replicas. SSD probability distributions were calculated using configurations saved each 1.0 ps from the 298 K simulation and stored for analysis. The biased probability density profile representing the probability of the peptide being located at designated values of SSD was constructed from the resulting biased-REMD trajectory results using an SSD bin width of 0.2 Å. The biased probability density profiles were then converted to non-biased probability distribution using Eq. 2. Once the non-biased probability density distributions were determined, the ΔA°_{ads} values were then calculated from Eq. 3. For statistical error estimation, five independent runs were generated for each system. Each of the independent runs included a separate evaluation of ΔA°_{ads} values after each successive 1.0 ns of sampling based on the cumulative set of trajectory data collected up to that point. This was done as a check for convergence, with sequential calculations of the ΔA°_{ads} values after each 1.0 ns resulting in random fluctuations about the average value after about 10 ns of biased-REMD. Similar steps were also applied for each of three independent runs of umbrella sampling.

2.2.3 *Interfacial Force Field Parameter-Set Tuning with Dual-Force Field CHARMM*

When ΔA°_{ads} values calculated from the biased-REMD simulations using the existing CHARMM parameters were

found to result in deviations of more than 1.0 kcal/mol from our experimental data, the Dual-FF CHARMM program was used to adjust the nonbonded parameters controlling interfacial behavior until the deviations were reduced to within 1.0 kcal/mol for all peptide-silica systems. As a general principle for this effort, we sought to develop an IFF parameter set with minimal changes to the nonbonded parameters while maximizing the overall agreement between the simulation and experimental values of adsorption free energy.

Our approach for tuning the nonbonded IFF parameter set began by identifying the parameters that were most suitable for tuning to adjust the ΔA°_{ads} values. The nonbonded interactions controlling the relative competition between the peptide and TIP3P water for the atoms of the silica surfaces consist of an electrostatic term represented by a Coulombic potential, with each atom in the system assigned a partial charge (q); and a 12-6 Lennard-Jones potential (LJ) to represent atom–atom overlap repulsion and vdW attraction, characterized by a well depth (ε) and interaction distance ($R_{\min}$). These potentials are represented with the forms:

$$v_{LJ}(r)_{ij} = \frac{q_i q_j}{4\pi\varepsilon_0 r_{ij}};$$
$$v_{LJ}(r)_{ij} = \varepsilon_{ij}\left[(R_{\min .ij}/r_{ij})^{12} - (R_{\min .ij}/r_{ij})^{6}\right] \quad (4)$$

where $v_{Coul}(r_{ij})$ is the potential energy from electrostatic interactions between atoms 'i' and 'j' separated by distance r_{ij}; q_i and q_j are the partial charges of atoms 'i' and 'j', respectively; ε_o is the permittivity of free space; $v_{LJ}(r_{ij})$ is the potential energy from LJ interactions between atoms 'i' and 'j' separated by distance r_{ij}; ε is the well depth of the LJ potential; and $R_{\min .ij}$ is the separation of the atoms when the LJ potential equals zero (an effective atomic radius).

To measure the extent that relative adjustment in these two different potential energy components could influence the ΔA°_{ads} values, two separate MD simulations with umbrella sampling were run using Dual-FF CHARMM. One simulation was performed with the partial charges of all surface atoms set to zero, so that electrostatic interactions between the atoms of the peptide (and solution) and the surface atoms were zero, thus effectively eliminating electrostatic interactions at the interface, leaving adsorption behavior to be totally driven by the LJ parameters. In a separate MD simulation, the LJ well-depth (ε) values of the surface atoms were set to very small values (~10^{-4} kcal/mol) for peptide–surface (and solution–surface) interactions, thus making the vdW contribution negligibly small while retaining sufficient atomic repulsion to avoid atom–atom overlap. These simulations effectively removed van der Waals attraction effects on adsorption, leaving peptide adsorption behavior to be dominated by electrostatic interactions. The PMF profiles resulting from these two separate umbrella sampling simulations were compared with the PMF profile for MD simulations conducted with the nonbonded parameters kept at their standard values, providing insight into the relative importance of electrostatic and vdW interactions for peptide adsorption. These relationships then served as a guide regarding which of these two types of nonbonded interactions could be modified to most effectively adjust peptide adsorption behavior to bring the calculated values of adsorption free energy in line with the experimental values.

As a further strategy to adjust peptide adsorption behavior, if adsorption was found to be consistently too strong or weak for all of the peptides, our approach was to first adjust the nonbonded parameters controlling the interaction between TIP3P water and the silica surfaces, since these changes would then be expected to have a similar effect on the adsorption behavior of each of the peptides. (We emphasize again that this adjustment in the IFF affects only the water–surface interaction; water–water and water–peptide interactions remain unchanged.) Accordingly, TIP3P water IFF parameters can be modified to minimize the root-mean-square deviation between the calculated and experimental values of free energy, after which the IFF parameters of the silica surface and/or individual amino acids could be subsequently modified to further minimize deviations in the adsorption free energies for individual peptides.

We note that the IFF parameter set derived by this approach does not represent a unique parameter set, and that variations in the specific order of the steps taken for the parameter tuning would result in different parameter sets, which serve to optimize the agreement between experiment and simulation. This current study is restricted to the use of eight host–guest peptides, which were chosen based on the intention of including each representative class of amino acid. Additional sets of experimental adsorption free energies from experiment and simulation using host–guest peptides with other choices of amino acid residues for X are expected to provide further validation for the present parameter set and extend the tuned parameter set for more general applicability.

3 Results and Discussion

3.1 Peptide Adsorption Free Energy on Silica Surfaces

3.1.1 Experimental Measurement of Adsorption Free Energies

Using the correlation between F_{des} versus ΔG°_{ads} [30], mean F_{des} values for each peptide–surface system measured by our standardized AFM method were translated into effective values of ΔG°_{ads}. Results from these correlations are

presented in Tables 2 and 3 for the quartz (100) and the silica glass surfaces, respectively.

3.1.2 Calculation of Adsorption Free Energies by Molecular Simulation

Using the existing CHARMM parameter set, estimates of the ΔA°_{ads} values were calculated from the PMF profiles obtained by umbrella sampling for each of the eight host–guest peptide systems on both the quartz (100) and silica glass surfaces.

Table 2 Adsorption free energies based on MD with umbrella sampling for TGTG-X-GTGT peptides on a quartz (100) surface using available CHARMM parameters

-X-	Adsorption free energy (kcal/mol)	
	Exp.[a]	Sim.[b]
Asn (N)	−1.3 (0.9)	−7.2
Asp (D)	−0.5 (0.9)	−7.5
Gly (G)	−1.0 (0.9)	−7.7
Lys (K)	−1.5 (0.9)	−6.6
Phe (F)	−0.7 (0.9)	−9.1
Thr (T)	−0.2 (0.9)	−6.0
Trp (W)	−0.6 (0.9)	−13.0
Val (V)	−0.3 (0.9)	−6.1

Experimental values are given as: Mean (95 % confidence interval)

[a] 95 % confidence interval for experimental data obtained from confidence intervals about linear regression line used for the correlation between F_{des} measured by AFM and ΔG°_{ads} determined by SPR

[b] Adsorption free energy values for (100) quartz were calculated from a single 3 ns umbrella simulation using default CHARMM parameters. Multiple independent simulations were not performed due to a decision to not proceed with tuning IFF parameters for this surface at this time. Confidence intervals are expected to be approximately $\sqrt{3}$ larger than those obtained for the silica glass surface using 3 independent simulations, shown in Table 3

Table 3 Adsorption free energies for TGTG-X-GTGT peptide on silica glass surface using available CHARMM parameters and the tuned IFF parameter set

-X-	Adsorption free energy (kcal/mol)		
	Exp.[a]	CHARMM param.	Tuned IFF param.
Asn (N)	−1.8 (0.9)	−10.5 (7.9)	−2.1 (0.5)
Asp (D)	−0.5 (0.9)	−7.6 (4.5)	−0.8 (0.4)
Gly (G)	−1.9 (0.9)	−8.2 (3.5)	−1.7 (0.7)
Lys (K)	−2.0 (0.9)	−9.7 (0.7)	−2.0 (0.3)
Phe (F)	−1.2 (0.9)	−6.2 (2.0)	−1.4 (0.5)
Thr (T)	−0.7 (0.9)	−8.9 (4.7)	−1.3 (0.4)
Trp (W)	−0.9 (0.9)	−9.0 (3.7)	−1.2 (0.4)
Val (V)	−0.7 (0.9)	−9.0 (4.0)	−1.1 (0.4)

The results are given as: Mean (±95 % confidence interval)

[a] 95 % confidence interval for experimental data obtained from confidence intervals about linear regression line used for the correlation between F_{des} measured by AFM and ΔG°_{ads} determined by SPR

The values for peptide adsorption on the quartz (100) and silica glass surfaces are given in Tables 2 and 3, respectively, along with the corresponding experimentally measured values of ΔG°_{ads}. As shown from these results, the ΔA°_{ads} values calculated from MD simulation using the CHARMM parameters for each of these surfaces were greatly overestimated (i.e., binding affinities are too strong) by about 5–9 kcal/mol relative to the experimental values. The experimental values are all between −2.0 and −0.2 kcal/mol, exhibiting relatively weak peptide adsorption behavior, while the simulations predict very strong adsorption, of −6.0 kcal/mol or stronger in every case. The results from these simulations were surprising given that the CHARMM parameters used for both the quartz (100) [21] and silica surfaces [23] were previously optimized for their interaction with TIP3P water. These results thus emphasize the difficulty in properly representing peptide adsorption behavior in aqueous solution because of its strong dependence on the *relative* balance between the affinity of solvent molecules (i.e., water and counter-ions) and amino acid residues of a peptide or protein for the adsorbent surface, and the importance of validating simulation results against carefully matched experimental values.

As noted above, the primarily objective of this present study was to modify and validate IFF parameters between amino acids and surfaces to support the ability to subsequently perform simulations of actual protein adsorption behavior for comparison with matched experimental studies, which are being conducted in parallel with these simulations. Due to the weak interactions of amino acid residues with the quartz (100) surface (more than half of which are not statistically distinguishable from zero at the 95 % confidence level in the experimental results presented in Table 2), it was determined by our experimental group that the adsorption of small proteins, such as lysozyme (14 kDa) to the quartz (100) surface was insufficiently strong to enable our subsequently planned experimental methods for the characterization of adsorbed protein orientation, conformation, and bioactivity to be successfully applied. For this reason, simulations of peptide adsorption on quartz (100) were not continued beyond the umbrella sampling results presented in Table 2, and focus was placed solely on the development of a tuned nonbonded IFF parameter set for peptide and protein adsorption on silica glass. IFF tuning for peptide interactions with the quartz (100) surface thus remains as future work.

3.2 Interfacial Force Field Parameter-Set Tuning

In preparation for tuning the nonbonded IFF parameters to correct the large differences in adsorption free energy

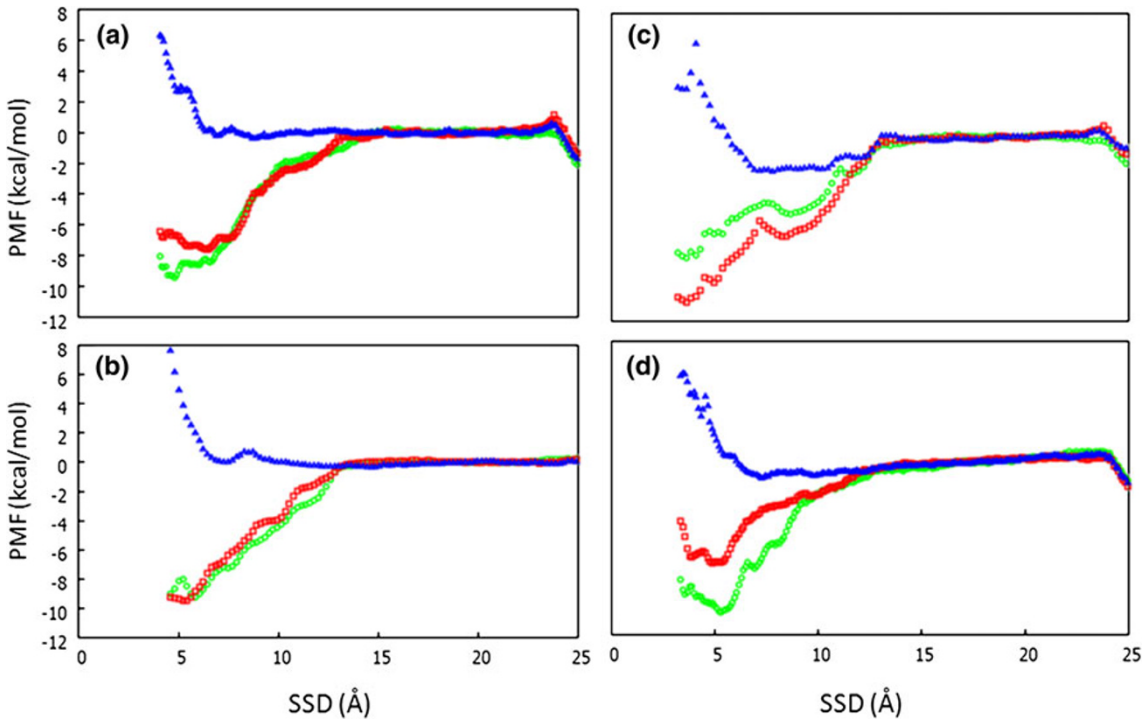

Fig. 2 Potentials of mean force (PMF) as a function of surface separation distance (SSD) for TGTG-X-GTGT peptides on the silica glass surface shown as three separate *curves* in each plot: based on (i) unmodified Lennard-Jones (LJ) (vdW) and Coulomb (electrostatic) parameters (*green circles*) using the existing CHARMM parameter set; (ii) vdW only (i.e., zero charge on surface atoms; *red squares*); and (iii) electrostatics only (i.e., LJ well-depth (ε)<<kT on surface atoms; *blue triangles*) for (**a**) X = Phe (F), (**b**) X = Trp (W), (**c**) X = Val (V), and (**d**) X = Lys (K)

compared to the experimental values, umbrella sampling simulations were first conducted using the Dual-FF CHARMM program to separate the contributions of electrostatic and vdW effects to evaluate their relative influence on peptide adsorption behavior to the silica surface. Examples of these PMF plots are presented in Fig. 2 for the cases of X = F, W, V, and K. PMF profiles for the other peptides were found to be qualitatively similar in appearance. It is evident from these plots that the PMF profiles, and hence the resulting ΔA°_{ads} values, are dominated by the vdW component of the nonbonded interactions between surface atoms and the peptide, with very little contribution from electrostatic effects. These results are intuitively understandable given that the highly polar nature of water enables it to outcompete the peptide for hydrogen-bondable hydroxyl groups presented by the silica glass surface, thus inhibiting peptide adsorption.

Having established that the overestimation of the adsorption free energy is primarily due to the vdW component of the peptide-surface nonbonded interactions, we performed a series of studies using umbrella sampling to investigate how to adjust the nonbonded parameters controlling peptide adsorption behavior to weaken the relative strength of vdW attraction of the peptides to the surface. As a general strategy, we first decreased the values of ε for the Si, O, and H atoms of the silica surface to weaken the overall dominance of the vdW effects for peptide adsorption. However, making the ε values smaller in magnitude for the atoms of the silica surface also decreases the vdW component of its nonbonded interactions with TIP3P water as well. To compensate for this effect and help shift the dominance of the nonbonded interactions from being controlled by vdW to electrostatic effects, we also increased the magnitude of the partial charges of the TIP3P water. We then also increased the magnitude of the ε parameter for interactions between the O and H atoms of the TIP3P water and the silica surface, to further increase the vdW attractive interactions of the water with the surface relative to those of the peptides. The nonbonded parameters of the atoms of the TIP3P water and silica glass surface were thus iterated, repeating the umbrella sampling calculation of adsorption free energy values until the calculated and experimental values were acceptably close. From this series of studies, the agreement between the calculated and experimental values of adsorption free energy for seven of the eight host–guest peptides was reduced to well within 1.0 kcal/mol. The final set of parameter values reflected a 35 and 14 % increase in the ε values and the magnitude of the partial charges, respectively, of TIP3P water, and a 40 % decrease in the ε values of the atoms of the silica glass (see Table 4).

Table 4 Summary of tuned IFF parameters (compared with the default values) required to bring adsorption free energies of the set of host–guest peptides into agreement with experiment for the silica glass surface

Residue	Atom type (IUPAC name)	LJ (ε)		Partial charge	
		CHARMM	Tuned	CHARMM	Tuned
TIP3P	OT	−0.1521	−0.2053	−0.834	−0.950
	HT	−0.0460	−0.0621	0.417	0.475
Trp	CY (CG)	−0.0700	−0.0350	−0.030	−0.030
	CA (CD1, CE3, CZ3, CZ2, CH2)	−0.0700	−0.0350	−0.115	−0.115
	HP (HD1, HE3, HZ3, HZ2, HH2)	−0.0300	−0.0150	0.115	0.115
	NY (NE1)	−0.2000	−0.1000	−0.610	−0.610
	H (HE1)	−0.0460	−0.0230	0.380	0.380
	CPT (CD2)	−0.0900	−0.0450	−0.020	−0.020
	CPT (CE2)	−0.0900	−0.0450	0.130	0.130
Silica	Si	−0.3000	−0.1800	0.900	0.900
	O	−0.1500	−0.0900	−0.450	−0.450
	O (H)	−0.1521	−0.0913	−0.660	−0.660
	H	−0.0460	−0.0276	0.430	0.430

For Trp, the IUPAC atom names as they appear in the CHARMM22 topology file are also given

IUPAC international union of pure and applied chemistry

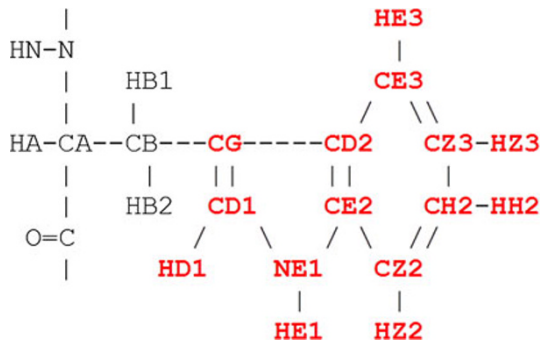

Fig. 3 Trp residue with IUPAC names as it appears in a conventional CHARMM22 topology file. Atom names in *red* indicate atoms for which the nonbonded van der Waals well depth parameters (ε) were tuned in this study

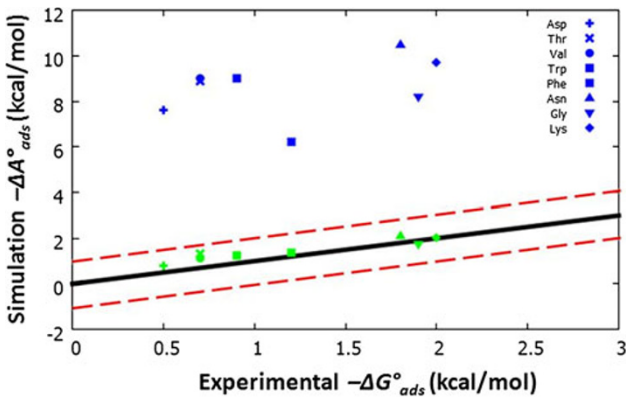

Fig. 4 Comparison of $-\Delta G^{\circ}_{ads}$ values from experiment and $-\Delta A^{\circ}_{ads}$ values from the simulations based on the initial CHARMM parameter set (*blue symbols* in y-axis range from 6 to 11 kcal/mol) and the final tuned IFF parameter set (*green symbols*, all within about 0.5 kcal/mol of the experimental values). The *solid black line* represents perfect agreement between simulation and experimental values of adsorption free energy. The *dashed red lines* represent deviations of ±1.0 kcal/mole around the *solid black line*, which we designated as the maximum tolerable deviation from the experimental values

Despite the above described parameter changes, the adsorption affinity for the host–guest peptide with X = W (Trp, tryptophan) to the silica glass surface was determined to still be about 2.5 kcal/mol too strong. This final deviation was then adjusted by decreasing the ε values of atoms of the indole ring of the side-chain of the Trp residue in the CHARMM amino acid library for interphase interaction with the silica surface by 50 %. With this modification, the ΔA°_{ads} value based on umbrella sampling was found to be well within the 1.0 kcal/mol targeted range of the experimental value. Figure 3 provides a schematic view of the Trp residue, showing specific IUPAC atom names as they appear in a standard CHARMM22 topology file, and atoms for which the vdW ε values were tuned. Table 4 provides the final set of tuned Trp parameters from this study along with the standard CHARMM parameters for comparison.

Biased-REMD simulations were subsequently conducted using the tuned parameter set, from which a final accurate set of ΔA°_{ads} values were calculated, which are presented in Table 3. Figure 4 presents the data in graphical form, emphasizing the reduction of deviation in the adsorption free energies obtained from our final set of biased-REMD simulations using the tuned IFF parameter

set compared to the values based on simulations with the CHARMM22/CMAP protein force field and previously published CHARMM parameters for silica glass, and showing that the adsorption free energies obtained using the tuned IFF are all well within the 1.0 kcal/mol targeted range of the experimental values.

It should be understood that the developed IFF force field parameters have been tuned in an *ad hoc* manner for the sole purpose of matching calculated peptide adsorption free energies to the experimentally measured values. The conformation of adsorbed peptides is obviously another very important characteristic of peptide adsorption behavior, which we were not able to address in the present study due to a lack of quantitative experimental data that can be used to evaluate simulation results. Further studies are planned, however, to apply the tuned IFF for the simulation of the adsorption behavior of small proteins, such as lysozyme, on a silica glass surface for which we are also generating experimental data on adsorbed protein conformation. Comparisons of adsorbed protein conformation between the simulation and experimental results will provide an assessment of the tuned IFF's ability to yield realistic predictions of adsorbed protein conformational behavior as well as energetics.

Although IFF parameters for peptide adsorption have not yet been developed for the quartz (100) surface, given the similarity between quartz and silica glass, we expect that the IFF parameters tuned for the silica glass should represent a substantial improvement for simulation of peptide and protein adsorption to quartz surfaces, compared to parameters that have been previously published based upon interactions between a quartz surface and water alone.

4 Conclusions

Adsorption free energies for a set of eight host–guest peptides over quartz (100) and amorphous silica surfaces were calculated from umbrella sampling and biased-REMD simulations using the CHARMM22/CMAP protein force field and CHARMM parameters previously published for both quartz and silica glass surfaces. Adsorption free energies were found to be overestimated for peptide adsorption to both of these surfaces by 5–9 kcal/mol relative to experimental values determined by AFM. The Dual-FF CHARMM program was used to adjust nonbonded parameters controlling peptide adsorption behavior in order to bring the adsorption free energies obtained by the simulations to well within a 1.0 kcal/mol of the experimental values, thus establishing a set of IFF parameters for peptide adsorption to silica glass. Subsequent studies are planned to apply this IFF parameter set to simulate the adsorption of small proteins to silica glass surfaces, for which paired experimental studies are also being carried out to assess the results of the protein adsorption simulations.

If successful, the Dual-FF code and tuned IFF force field improve the potential for molecular simulation to help understand and predict protein adsorption behavior at the atomic level and to be used as a design tool for system optimization for numerous applications in biomedical engineering, biotechnology, and biodefense.

Acknowledgments This project received support from the Defense Threat Reduction Agency-Joint Science and Technology Office for Chemical and Biological Defense (Grant no. HDTRA1-10-1-0028). Computing resources: Palmetto Linux Cluster, Clemson Univ. The authors thank Dr. Charles L. Linden Jr., Paradox Technologies, Valparaiso, FL for biodefense technical consulting support, and Dr. Christopher Lorenz of Kings College, London, UK. and Dr. Gary S. Grest of Sandia National Labs for providing assistance in the development of the molecular model of the amorphous silica glass surface. We also thank Ms. Megan Grobman, Dr. Lara Gamble, and Dr. David Castner of NESAC/BIO at the University of Washington for assistance with surface characterization with XPS under the funding support by NIBIB (Grant # EB002027).

References

1. Castner DG, Ratner BD (2002) Surf Sci 500:28–60
2. Hlady V, Buijs J (1996) Curr Opin Biotechnol 7:72–77
3. Latour RA (2005) The encyclopedia of biomaterials and bioengineering. Taylor & Francis, New York
4. Tsai WB, Grunkemeier JM, McFarland CD, Horbett TA (2002) J Biomed Mater Res 60:348–359
5. Blasi P, Glovangnoli S, Schoubben A, Ricci M, Rossi C (2007) Adv Drug Deliv Rev 59:454–477
6. Dobrovolskaia MA, Mcneil SE (2007) Nat Biotechnol 2:469–478
7. Geelhood SJ, Horbett TA, Ward WK, Wood MD, Quinn MJ (2007) J Biomed Mater Res Part B Appl Biomater 81B:251–260
8. Lange K, Grimm S, Rapp M (2007) Sens Actuators B 125:441–446
9. Amanda A, Kulprathipanja A, Toennesen M, Mallapragada SK (2000) J Membr Sci 176:87–95
10. Mertz CJ, Kaminski MD, Xie YM (2005) J Magn Magn Mater 293:572–577
11. Graham LM, Bok Lee S, Nguyen TM (2011) Nanomedicine 6(5):921–928
12. Driks A (2009) Mol Aspects Med 30:368–373
13. Meng M, Stievano L, Lambert JF (2004) Langmuir 20:914–923
14. Willett RL, Baldwin KW, West KW, Pfeiffer LN (2005) Proc Natl Acad Sci USA 102:7817–7822
15. Oren EE, Tamerler C, Sahin D, Hnilova M, Safar Seker UO et al (2007) Bioinformatics 23:2816–2822
16. Gao Q, Xu WJ, Xu Y, Wu D, Sun YH et al (2008) J Phys Chem B 112:2261–2267
17. Lorenz CD, Crozier PS, Anderson JA, Travesset A (2008) J Phys Chem C 112:10222–10232
18. Notman R, Oren EE, Tamerler C, Sarikaya M, Samudrala R et al (2010) Biomacromolecules 11:3266–3274

19. Skelton AA, Fenter P, Kubicki JD, Wesolowski DJ, Cummings PT (1011) J Phys Chem C 115:2076–2088
20. Puddu V, Perry CC (2012) ACS Nano 10.1021/nn301866q
21. Lopes PE, Murashov V, Tazi M, Demchuk E, Mackerell ADJ (2006) J Phys Chem B 110:2782–2792
22. Litton DA, Garofalini SH (2001) J Appl Phys 89:6013–6023
23. Cruz-Chu ER, Aksimentiev A, Schulten K (2006) J Phys Chem B 110:21497–21508
24. Vellore NA, Yancey JA, Collier G, Latour RA, Stuart SJ (2010) Langmuir 26:7396–7404
25. Costa D, Tougerti A, Tielens F, Gervais C, Stievano L et al (2008) Phys Chem Chem Phys 10:6360–6368
26. Nonella M, Seeger S (2008) Chem Phys Chem 9:414–421
27. Rimola A, Sodupe M, Ugliengo P (2009) J Phys Chem C 113:5741–5750
28. Wei Y, Latour R (2009) Langmuir 25:5637–5646
29. Wei Y, Latour RA (2008) Langmuir 24:6721–6729
30. Thyparambil AA, Wei Y, Latour RA (2012) Langmuir 28: 5687–5694
31. Wei Y, Latour RA (2010) Langmuir 26:18852–18861
32. Wang F, Stuart SJ, Latour RA (2008) Biointerphases 3:9–18
33. O'Brien CP, Stuart SJ, Bruce DA, Latour RA (2008) Langmuir 24:14115–14124
34. MacKerell AD, Bashford D, Bellott M, Dunbrack RL, Evanseck JD et al (1998) J Phys Chem B 102:3586–3616
35. Mackerell AD, Feig M, Brooks CL (2004) J Comput Chem 25:1400–1415
36. Biswas PK, Vellore NA, Yancey JA, Kucukka IT, Collier G (2012) J Comp Chem 33:1458–1466
37. Sumner AL, Menke EJ, Dubowski Y, Newberg JT, Penner RM et al (2004) Phys Chem Chem Phys 6:604–613
38. Kurokawa A, Odaka K, Azuma Y, Fujimoto T, Kojima I (2009) J Surf Anal 15:337–340
39. Cras JJ, Rowe-Taitt CA, Nivens DA, Ligler FS (1999) Biosens Bioelectron 14:683–688
40. Skłodowska A, Woźniak M, Matlakowska R (1999) Biol Proced Online 1:114–121
41. Bowman C (1998) Cell Biochem Biophys 29:203–223
42. Szymczyk K, Jańczuk B (2008) Langmuir 24:7755–7760
43. Brooks BR, Bruccoleri RE, Olafson BD, States DJ, Swaminathan S et al (1983) J Comput Chem 4:187–217
44. Plimpton SJ (1995) J Comp Phys 17:1–19
45. Lorenz CD, Tsige M, Rempe SB, Chandross M, Stevens MJ et al (2010) J Comput Theor Nanos 7:2586–2601
46. Yancey JA, Vellore NA, Collier G, Stuart SJ, Latour RA (2010) Biointerphases 5:85–95
47. Nose S, Klein ML (1983) Mol Phys 50:1055–1076
48. Nose S (1984) Mol Phys 52:255–268
49. Andersen HC (1983) J Comput Phys 52:24–34
50. Raut V, Agashe M, Stuart SJ, Latour RA (2005) Langmuir 21:1629–1639
51. Sugita Y, Okamoto Y (1999) Chem Phys Lett 314:141–151
52. Beutler TC, Vangunsteren WF (1995) Chem Phys Lett 237: 308–316
53. Harvey SC, Prabhakaran M (1987) J Phys Chem 91:4799–4801
54. Mezei M (1987) J Comput Phys 68:237–248
55. Torrie GM, Valleau JP (1977) J Chem Phys 66:1402–1408
56. Torrie GM, Valleau JP (1977) J Comput Phys 23:187–199
57. Kumar S, Bouzida D, Swendsen RH, Kollman PA, Rosenberg JM (1992) J Comput Chem 13:1011–1021
58. Overbeek JTG (1977) J Colloid Interface Sci 58:408–422
59. Mezei M, Beveridge D (1986) Ann N Y Acad Sci 482:1–23